Acta Geodyn. Geomater., Vol. 19, No. 4 (208), 281–290, 2022
DOI: 10.13168/AGG.2022.0013
journal homepage: https://www.irsm.cas.cz/acta

ORIGINAL PAPER

EMPIRICAL MODE DECOMPOSITION FOR POST-PROCESSING THE GRACE MONTHLY GRAVITY FIELD MODELS

Changmin HUAN [1], Fengwei WANG [2] and Shijian ZHOU [3] *

[1] *College of Surveying and Mapping Engineering, East China University of Technology, Nanchang, PR, China*
[2] *State Key Laboratory of Marine Geology, Tongji University, Shanghai, PR, China*
[3] *Nanchang Hangkong University, Nanchang, PR, China*

**Corresponding author's e-mail:* 408608628@qq.com

ARTICLE INFO

Article history:
Received 28 August 2022
Accepted 24 November 2022
Available online 16 December 2022

Keywords:
GRACE
Time variable gravity
Empirical Mode Decomposition
Filtering

ABSTRACT

Considering the advantage of Empirical Mode Decomposition (EMD) for extracting the geophysical signals and filtering out the noise, this paper will first apply the EMD approach to post-process the Gravity Recovery and Climate Experiment (GRACE) monthly gravity field models. A 14-year time-series of Release 06 (RL06) monthly gravity field models from the Center for Space Research (CSR) truncated to degree and order 60 from the period April 2002 to August 2016 are analyzed using the EMD approach compared with traditional Gaussian smoothing filtering. Almost all fitting errors of GRACE spherical harmonic coefficients by the EMD approach are smaller than those by Gaussian smoothing, indicating that EMD can retain more information of the original spherical harmonic coefficients. The ratios of latitude-weighted RMS over the land and ocean signals are adopted to evaluate the efficiency of eliminating noise. The results show that almost all ratios of RMS for the EMD approach are higher than those of Gaussian smoothing, with the mean ratio of RMS of 3.61 for EMD and 3.41 for Gaussian smoothing, respectively. Therefore, we can conclude that the EMD method can filter noise more effectively than Gaussian smoothing, especially for the high-degree coefficients, and retain more geophysical signals with less leakage effects.

1. INTRODUCTION

Due to some factors such as the influence of the GRACE satellite orbit error and instrument measurement error, there are some significant noise on the higher-degree terms of GRACE gravity field model (Wahr et al., 1998), which is represented by the north-south stripes. Therefore many filtering methods are developed to filter out the noise to extract the interesting geophysical signals, which normally can be divided into three categories: (1) isotropic filters, whose basic filtering principle is to suppress the noise by reducing the weight of high-degree coefficients, specifically including Gaussian smoothing (Wahr et al., 1998), Fan filtering (Zhang et al., 2009), RMS (root mean square) filtering (Chen et al., 2006), Wiener filtering (Sasgen et al., 2007), etc. Note that these filtering methods may be easily affected by the adopted parameters such as the smoothing radius. (2) anisotropic filters, which were developed to filter out the north-south stripes error by Swenson and Wahr (2006), then modified as P4M6 (Chen et al., 2007), P4M15 (Chamber et al., 2012), Duan (Duan et al., 2009), DDK filtering (Kusche et al., 2007). (3) Empirical orthogonal function (Kaihatu et al., 1998), which is a method to analyze the structural features in matrix data and extract the main data feature quantity (Weare et al., 1982). In geological data analysis, the feature vectors usually correspond to spatial samples, so they are also called spatial feature vectors or spatial modes. The principal component corresponds to the time change, also known as the time coefficient, which mainly includes principal component analysis (PCA, Rangelova et al., 2007), independent component analysis (ICA; Frappart et al., 2011; Guo et al., 2014), multichannel singular spectrum analysis (MSSA, Rangelova et al., 2012; Wang et al., 2020; Shen et al., 2021). The mentioned isotropic and anisotropic i.e., (1) and (2) approaches differ in filtering idea. Gaussian-type approach reduces the impact of short-wavelength component error by reducing the coefficient weight of higher-degree terms of the model, while de-correlational approach eliminates the correlation error between the odd and even terms of spherical harmonic coefficients by fitting polynomials (Guo et al., 2018).

Compared with those above filtering methods, the EMD method can adaptively extract periodic components of different frequencies and amplitudes which does not need to set the corresponding parameter such as the window size and reconstructed order for the MSSA approach, which are commonly used in many study fields, including geodesy for analyzing the GNSS (Global Navigation Satellite System) time series (Liu et al., 2021), studying changes in groundwater storage at different time scales (Xu et al., 2021), hydrology fields such as

Cite this article as: Huan C, Wang F, Zhou S: Empirical mode decomposition for post-processing the GRACE monthly gravity field models. Acta Geodyn. Geomater., 19, No. 4 (208), 281–290, 2022. 0. DOI: 10.13168/AGG.2022.0013

identifying the radon precursor anomalies in groundwater (Fu et al., 2016; Feng et al., 2022), sea level change (Lan et al., 2021), and so on. Most previous studies validated that the EMD method can better extract the signals during the procedure of filtering noise, which is considered to be a major breakthrough in the linear and steady-state spectral analysis based on the Fourier transform since 2000 and it is based on the time scale characteristics of the time series. There is no need to preset any basis functions, which makes it theoretically applicable to any type of signal decomposition. To the best authors' knowledge, the EMD approach has never been used in the GRACE filtering field. Therefore, we will apply the EMD for post-processing the spherical harmonic coefficients of the GRACE monthly gravity field model. The rest of this paper is organized as follows. Section 2 introduces the basic principle and application field of EMD. The signal extraction from the real GRACE spherical harmonics time series and global mass changes from the EMD and Gaussian filtering approaches are described in Section 3. The concluding remarks are presented in Section 4.

2. METHODOLOGY AND DATA

Empirical Mode Decomposition is a spectral class decomposition method, which can decompose a time series into several components such as trend, modulation oscillation, and noise (Braun et al., 2011). The EMD method will be first applied to filter the strong noise of the GRACE monthly gravity field models together with the Gaussian smoothing approach. There exist 17 missing monthly data in GRACE data during the period from April 2002 to August 2016. Before performing the EMD approach, we first interpolate the missing data using the cubic spline interpolation method similar to Guo et al. (2018).

2.1. GRACE GRAVITY FIELD SOLUTIONS

The Earth's gravity field is determined by the mass of the Earth's internal system and used to reflect the spatial distribution of the Earth's internal materials and external masses. The study of the Earth's temporal gravity field is not only one of the research directions of modern satellite geodesy, but also provides important spatial information for modern geophysical science to solve the problems of resources and environment (Cui et al., 2019). Due to the influence of the surface atmosphere, oceans, glaciers, and crustal deformation, the Earth's gravity field is constantly changing. Since 2002, the Gravity Recovery and Climate Experiment (GRACE) mission has provided essential information about Earth's gravity field changes, which allows to monitoring of the migration and redistribution of the Earth's surface mass (Tapley et al., 2004). It has been widely used by different scientific fields to study, among others: land water storage change. (Ramillien et al., 2008; Cazenave et al., 2010), glacier isostatic adjustment (Chen et al., 2009; Velicogna and Wahr, 2013; Gao et al., 2015), ocean mass change (Lu et al., 2015), regional crustal deformation (Wang et al., 2014), and so on. The spherical harmonic coefficient model data used in this paper is provided by CSR, and the expansion degree is 60. The coefficient does not include the degree-1 term, and the accuracy of the determined $C_{2,0}$ coefficient is relatively low. Generally, the corresponding the degree-1 term is added back and the $C_{2,0}$ coefficient is replaced when processing the calculation.

2.2. EMD APPROACH

EMD is an adaptive method for analyzing non-stationary and nonlinear time series (Huang et al., 1998; Qian et al., 2010; Lei et al., 2013; Colominas et al., 2014; Miao et al., 2011), which can be seen as a spectral-like decomposition method similar to the wavelet decomposition method (Boudraa et al., 2007). It has been commonly used to analyze various geophysical data, such as sea surface temperature (Wu et al., 2008) and surface air temperature (Qian et al., 2010), seasonal sea level cycles (Lan et al., 2021). It can decompose the original time series $x(t)$ into several IMF (intrinsic mode functions) components with a frequency from high to low and a residual term based on the local time scale of the signal and can adaptively generate basis functions. The specific procedures are as follows:

Step 1. To find the maximum and minimum values in the original series $x(t)$, form the upper and lower envelopes, and find their average values to form the average series $m(t)$. The difference between the original time series and the average series can be expressed as:

$$h(t) = x(t) - m(t), \tag{1}$$

Step 2. Repeat step 1 for k times, if the $h_k(t)$ fulfills two conditions, i.e.: (i) In the entire data segment, the number of extreme points and the number of zero-crossing points must be equal or the difference cannot exceed one at most. (ii) At any time, the average value of the upper envelope formed by the local maximum points and the lower envelope formed by the local minimum points is zero, that is, the upper and lower envelopes are locally symmetrical concerning the time axis (Zhang et al., 2017).

Therefore, each IMF contains lower frequency oscillations than those obtained before. The mean value of the upper and lower envelopes is zero. In the actual decomposition process, the second condition is difficult to satisfy and the threshold expression for stopping filtering for each component is as follows:

$$SD = \sum_{t=1}^{N} \left[\frac{| d_{k+1}(t) - d_k(t) |^2}{d_{k-1}^2(t)} \right], \tag{2}$$

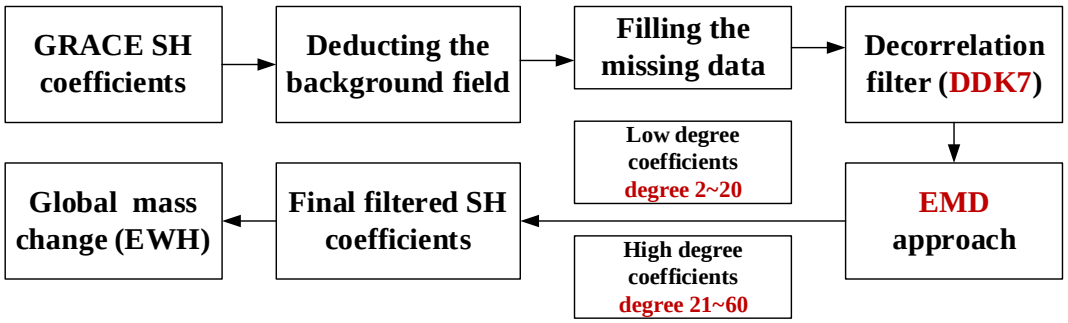

Fig. 1 The flow chart of EMD for filtering the GRACE SH coefficients.

where $d_k(t)$ and $d_{k-1}(t)$ are two adjacent data sequences in the IMF selection process and N represents the length of the time series, SD represents the threshold at which each IMF stops filtering, which is usually taken as a number between 0.2 and 0.3 (Huang et al., 1998)

Step 3. Subtract the first IMF from the original time series $x(t)$ to generate a new time series:

$$x_1(t) = x(t) - IMF_1(t), \tag{3}$$

Step 4. Take $x_1(t)$ as the original time series and perform all the above steps to obtain the m IMF components and a residual term. Finally, the original time series $x(t)$ can be represented as:

$$x(t) = \sum_{i=1}^{m} IMF_i(t) + r(t), \tag{4}$$

where m denotes the number of IMF components, $r(t)$ represents the residual term.

Normally the high-frequency components are recognized as noise, and the remaining components are used to reconstruct the signals. Therefore, it is valuable to determine the boundary point d between the noise and signal components. In this study, the power spectrum analysis method is adopted to determine the parameter d (Shu et al., 2007). Then the reconstructed signals $s(t)$ can be written as follows:

$$s(t) = \sum_{i=d}^{m} IMF_i(t) + r(t), \tag{5}$$

2.3. EMD FOR FILTERING GRACE MONTHLY GRAVITY FIELD SOLUTIONS

Considering the advantage of the EMD approach, we will first apply EMD method for filtering the GRACE monthly temporal gravity field solutions to validate whether it can better filter out noise and extract more useful geophysical signals. As we all know, stripe noise is often mixed with the low-frequency components related to signals, and needs to filter using the decorrelation filtering method before adopting the EMD and Gaussian smoothing. Here in this study, we adopt DDK7 filter first so as to remove the stripe noise in advance. Besides, the low-degree coefficients mainly contain real geophysical signals with less noise, however, the high-degree coefficients contain more noise. According to Yi et al. (2022), the spherical harmonic coefficients are divided into low-degree (degrees 2~20) and high-degree (degrees 21~60) parts, then filter the noise using the EMD and DDK7 method. When performing the EMD approach, each spherical harmonic coefficient will form a certain amount of eigenmode function (IMF) after being decomposed by the EMD method. Following Yi et al. (2022), we process the low-degree and high-degree parts separately. The criterion is set as follows: (1) the period of the low-degree part of the IMF component greater than 0.45 is taken to form the reconstructed signal, (2) the high-degree part of the IMF component with the period greater than 0.70 is selected after the experiment comparison. The flow chart of the EMD filtering method to process the GRACE gravity field SH coefficients is presented in Figure 1.

3. RESULTS AND ANALYSIS

3.1. RESULT IN THE SPECTRAL DOMAIN

We used the RL06 monthly gravity field model released by the Center for Space Research (CSR) from April 2002 to August 2016, with 17 missing months (9.8 % of the total months), and the cubic spline interpolation method is used to interpolate the missing months. The SH coefficients are truncated at maximum degree and order (d/o) 60 without the effects of atmosphere, ocean, and tide and deduct the average field from April 2002 to August 2016 (Cui et al., 2020). Decorrelation is an important step before the EMD filtering, therefore, the DDK7 filtering is adopted here. To better compare the performance of the EMD approach, the 300 km Gaussian smoothing method is further used through experimental analysis (Fig. 2). The fitting error of EMD and Gaussian smoothing approaches for each SH coefficient can be calculated as follows,

$$\sigma = \sqrt{\frac{1}{N}\sum_{t=1}^{N}(x(t) - s(t))^2} \tag{6}$$

where σ represents the fitting error, $s(t)$ represents the reconstructed SH signal after filtered by EMD and

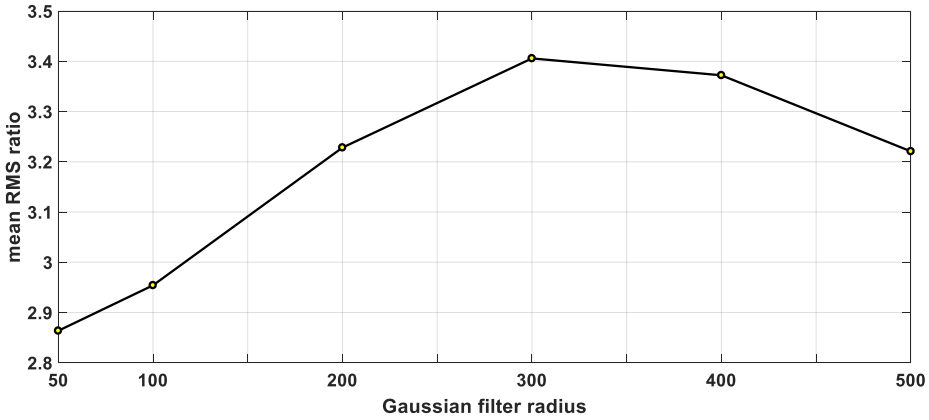

Fig. 2 Mean ratios of RMS for the combined filtering strategy (DDK7 and Gaussian smoothing) with different radiuses.

Gaussian smoothing, $x(t)$ is the original SH signal, and N represents the length of each SH coefficient series.

It can be seen from Figure 2 that, with the increasing Gaussian smoothing filtering radius, the average ratio of RMS gradually increases to a peak value, and then decreases. Based on this, we can conclude that Gaussian smoothing 300 km and DDK7 filtering method can better filter out noise with the highest ratio of RMS (3.41). Therefore, we finally select Gaussian smoothing with a filtering radius of 300 km for comparative analysis and processing. Here we take $C_{50,59}$ and $C_{60,60}$ SH coefficients as examples to show the comparison of the two filtering approaches. Figure 3 shows the component diagrams and power spectra of the eigenmode functions of $C_{50,59}$ and $C_{60,60}$. When we use the power spectrum analysis method to select the IMF components to reconstruct the signals, the period of an IMF is determined in such a way that the period corresponding to the point with the highest power is the major period since the IMFs are arranged from high to low frequencies after the EMD decomposition, and when it is determined that the period of an IMF meets the criterion mentioned in

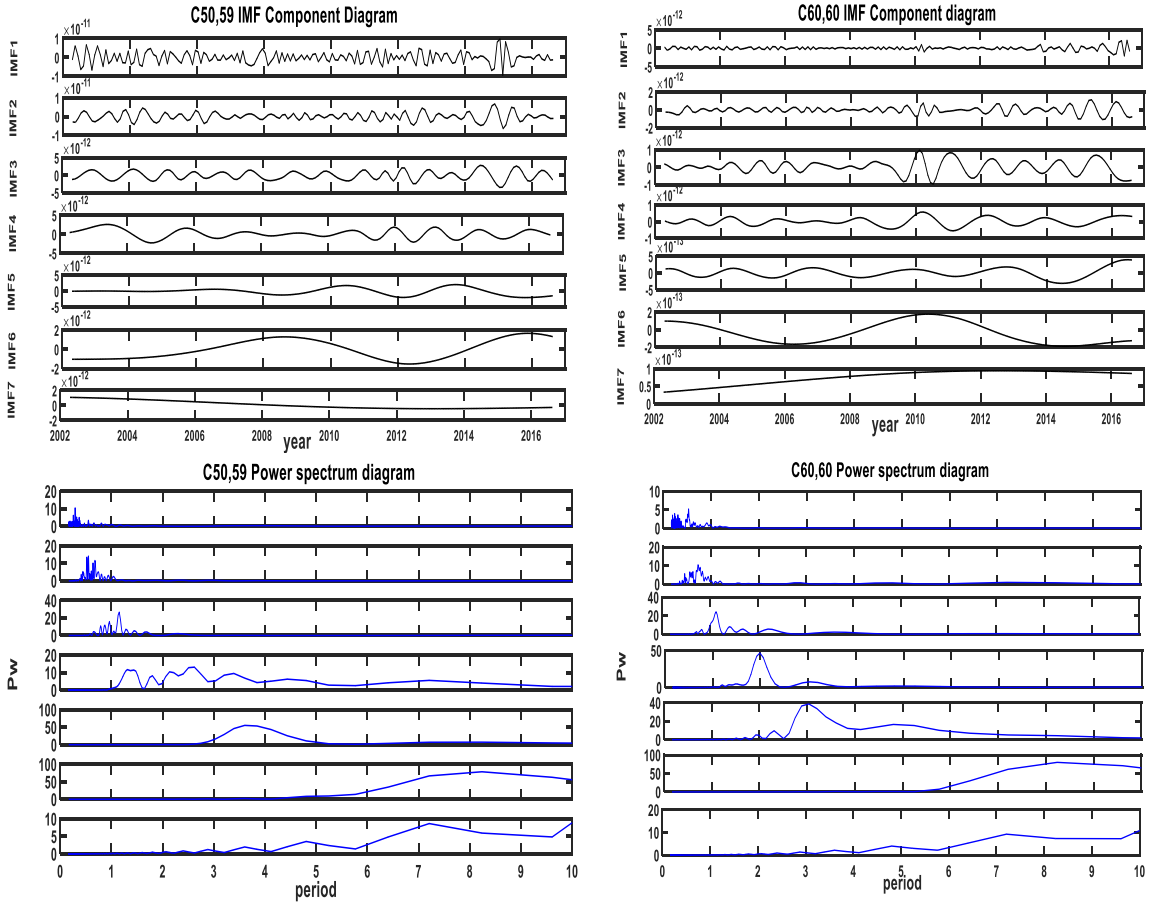

Fig. 3 Power spectrum and IMF component diagram of $C_{50,59}$ and $C_{60,60}$.

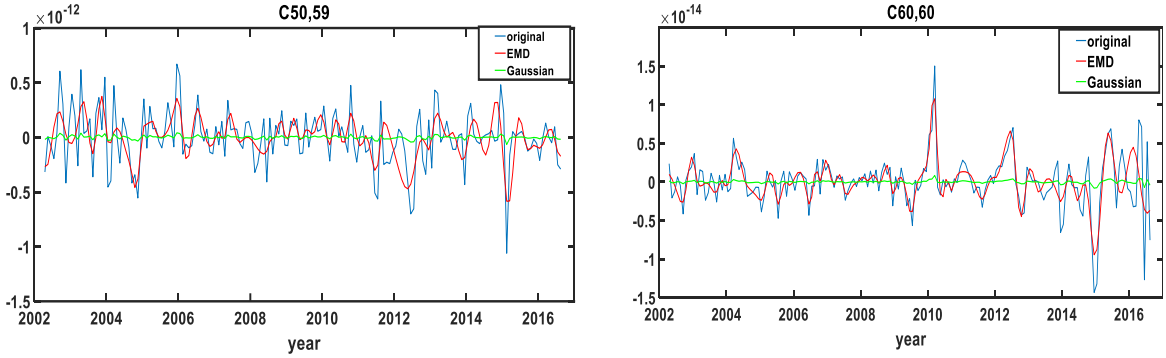

Fig. 4 The reconstructed coefficients after filtered by two approaches and original SH coefficients for $C_{50,59}$ and $C_{60,60}$.

Section 2.2, the reconstruction is taken from this IMF onwards. And the advantage of the EMD approach in this paper lies in the processing of the higher-order part (after 20 degree) of the time-varying gravity field model. In the case of Gaussian smoothing approach, the gravity field model is weighted. Moreover, Gaussian approach reduces the weight of the higher degree terms of the spherical harmonic coefficients to achieve the smoothing effect at the expense of resolution (Wahr et al., 1998). Thus, more of the real geophysical signal is lost. Consequently, we used two higher-degree coefficients. As the two high-degree coefficients are shown below, which are decomposed into 7 IMFs, and IMF1-IMF3 are the dominant semi-annual and annual periods, IMF4-IMF5 cycles are mainly 2.1 to 2.5 years, with long-period waves in the range 2.1 to 2.5 years also contributing to cyclical water storage changes (Schmidt et al., 2008).

Figure 4 presents the reconstructed signals extracted by the two methods and the original SH coefficients of $C_{50,59}$ and $C_{60,60}$. We can find that the amplitude of the reconstructed coefficients after EMD filtering is more consistent with the amplitude of the coefficients of the original signal, while the amplitude of the reconstructed coefficients after Gaussian smoothing differs significantly from the amplitude of the coefficients of the original signal and has lost its original fluctuation range mainly due to the smaller weights for high degree SH coefficients. The reason why we choose these two coefficients is that the EMD filtering method can better show its advantages in the high-degree part, so we choose these two high-degree coefficients with good effects for display. To clearly compare the difference between the EMD and Gaussian smoothing methods, Figure 5 shows the amplitude of each SH coefficient of the original data of March 2016, the amplitude of each coefficient after EMD filtering and Gaussian filtering, and the difference in amplitude before and after filtering.

The original amplitudes of all SH coefficients in March 2016 are shown in Figure 5(a) with the unreasonably large values in the high degree, which is the main cause of the north-south stripes and high-frequency noise. From Figure 5(b) and (d), it can be concluded that EMD can retain more information in the high-degree part relative to the Gaussian smoothing, which also suppresses the signals while filtering out the noise. Comparing Figures 5(c) and 5(e), we can find that the noise mainly exists in the part with the degree higher than 20, and the part with the degree lower than 20 contain less noise. It noticed that the amplitude magnitude of the low-degree part after EMD filtering is especially close to the original data. Moreover, the high-degree coefficients are closer to the original data than the Gaussian smoothing method.

Then we calculate the fitting errors of all GRACE SH coefficients shown in Figure 6. The fitting errors of $C_{50,59}$ and $C_{60,60}$ for EMD method is 2.10e-12 and 5.60e-13, respectively, while 3.54e-12 and 5.93e-13 for Gaussian smoothing method, indicating that EMD can retain more information of original SH coefficients than the Gaussian smoothing. And from Figure 6, we can find that almost all fitting errors of EMD are smaller than those of Gaussian smoothing, especially for the SH coefficients below degree 20, mainly because the IMF components lost by the EMD filtering in this part are fewer, therefore the reconstructed SH coefficients are close to the original time series. For the part higher than degree 20, the reconstructed components are determined based on the criteria introduced in Section 2.2. This part loses more IMF components than the SH coefficients below degree 20, but the fitting errors are still almost smaller than those of the Gaussian smoothing method. The results presented in Figure 5 and Figure 6 also emphasized that there is a difference between both filtering methods in terms of the noise filtering effect in the low-degree part, it emphasized that the EMD method can retain more signal and contain more information than the Gaussian smoothing method, whether the extracted more part is mainly related to signal or noise need further validation through the global mass change comparison.

3.2. GLOBAL MASS CHANGE COMPARISON

To further validate the performance of EMD compared to Gaussian smoothing, we chose January

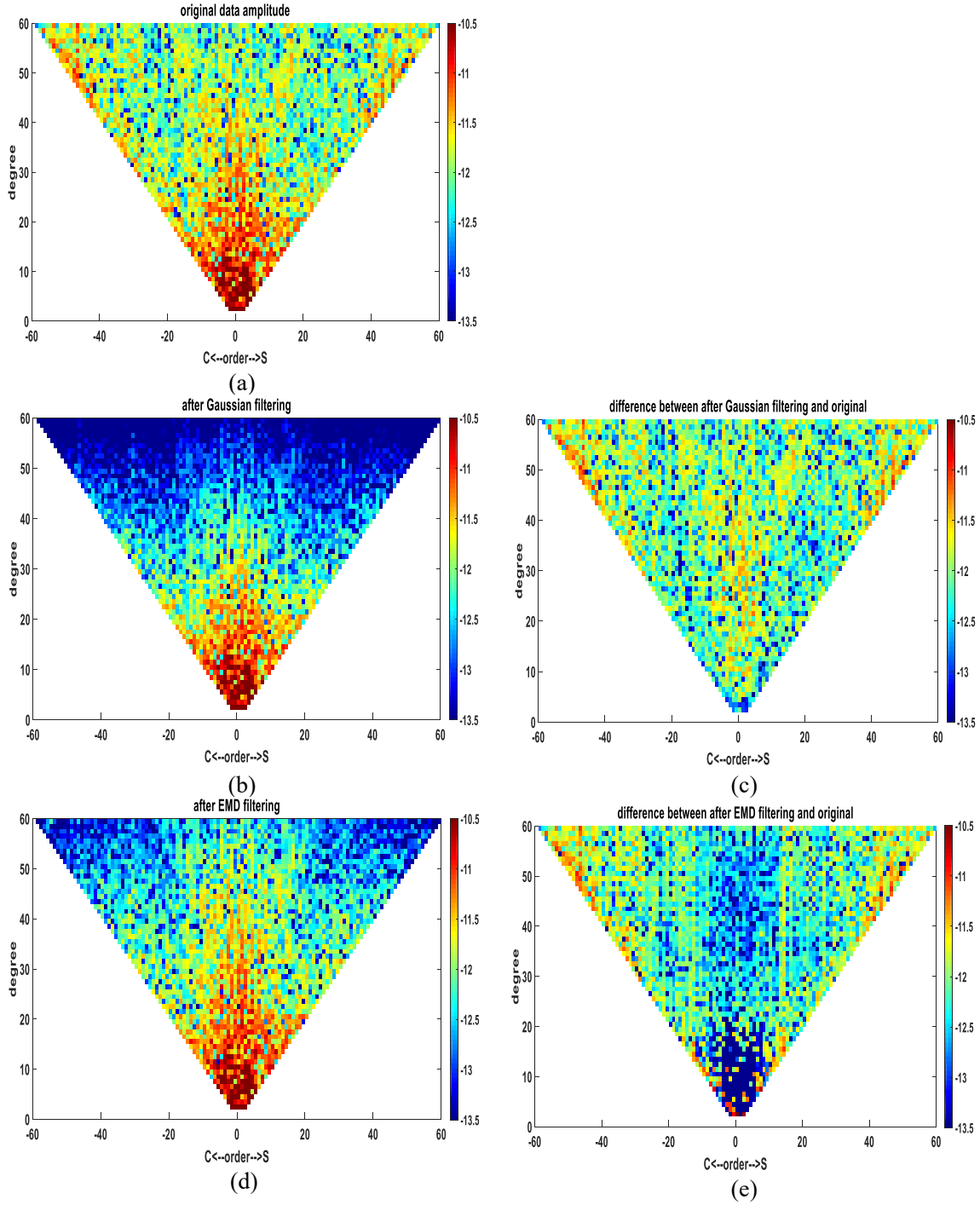

Fig. 5 The amplitude of each SH coefficient of the original data and the amplitude of each coefficient after EMD and Gaussian filtering, and their differences in March 2016. (a) no filtering (b) Gaussian smoothing (c) the noise filtered by Gaussian smoothing (d) EMD (e) the noise filtered by EMD (in log10).

2014 and March 2016 as an example for analysis. We converted the filtered GRACE SH coefficients by EMD and Gaussian smoothing approach to a grid map of $1^{\circ} \times 1^{\circ}$ EWH (Equivalent water height). Figure 7 shows the spatial inversion map after EMD filtering and Gaussian smoothing. It can be seen that there exists a serious north-south stripe error without filtering (shown in Figure 7(a) - 7(b)), which will seriously mask the real signal, which is not conducive to extracting the real geophysical signal. Besides, Figure 7(c) - 7(d) present the global mass changes after DDK7 and EMD filtering, (e) and (f) are those of DDK7 and 300-km Gaussian smoothing. Note that (g) and (h), (i), (j) are the filtered noise by EMD and 300 km Gaussian filtering, respectively. And we can see from the sub-figures (c), (d) and (e), (f) of Figure 7 that the combination of DDK7 & EMD filtering can more effectively remove the north-south stripe error,

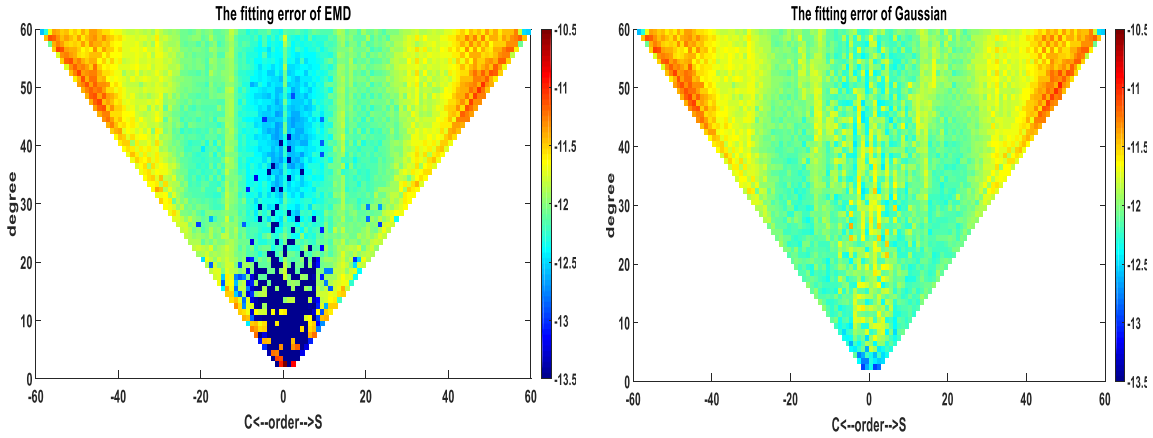

Fig. 6 The fitting errors of EMD (left) and 300-km Gaussian smoothing (right) approach (in log10).

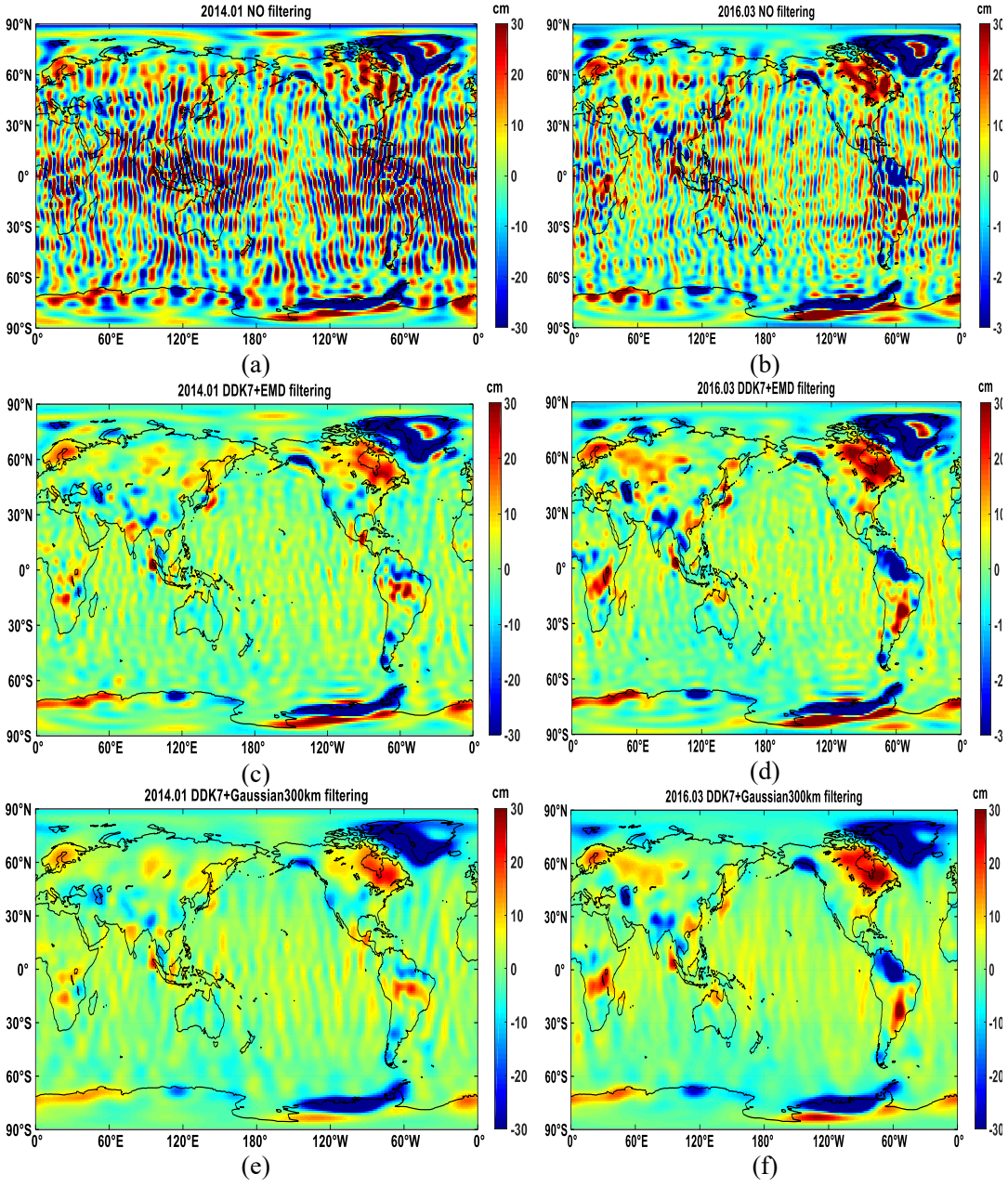

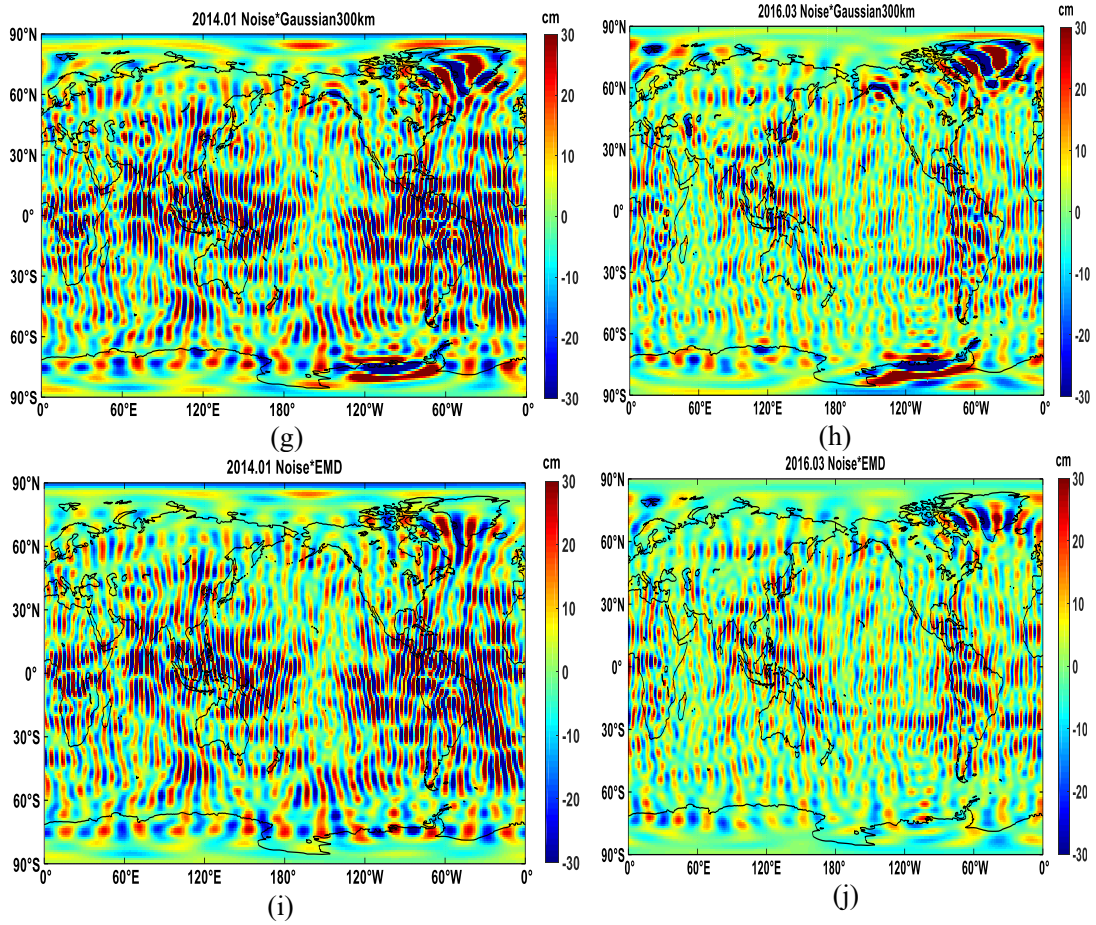

Fig. 7 The global mass change comparison after filtered by EMD and 300-km Gaussian smoothing and the corresponding noise for January 2014 and March 2016.

Table 1 The ratios of RMS for EMD and Gaussian smoothing filtering for January 2014 and March 2016.

Index	2014.01	2016.03
EMD	3.88	4.78
Gaussian smoothing (300-km)	2.88	3.42

and the retained signal is stronger, and also can infer the leakage error of the EMD method is weaker than that of the Gaussian smoothing. It can be concluded that the EMD method can retain more geophysical signals in Greenland, Antarctic and Arctic regions with less leakage signals.

Besides, we used the latitude weighted root mean square (RMS) ratio to accurately evaluate the denoising effect. This is mainly based on the fact that the surface mass of the whole land varies more than the oceans, in addition to the C_{20} term, the variable ratio is the ratio of latitudinal weighted root mean square (RMS) values on land and ocean signals (Chen et al., 2006). To reduce the leakage of signals from land, only ocean points more than 300 km from the coast are included.

$$RMS\_Ratio = \frac{RMS(MASS_{land} + Err)}{RMS(MASS_{ocean} + Err)}, \quad (7)$$

where $MASS_{land}$ and $MASS_{ocean}$ represent *respectively* the signals on land and ocean, and Err is the noise.

As shown in Table 1, the ratio of RMS of January 2014 and March 2016 are 3.88 and 4.78 for EMD, 2.88 and 3.42 for 300 km Gaussian smoothing. The relative improvements of the ratio of RMS of the EMD method are 34.7 % and 39.8 % for January 2014 and March 2016 with respect to the Gaussian smoothing, respectively.

We noticed that almost all ratios of RMS for EMD method are higher than those of the Gaussian smoothing method (Fig. 8). The mean ratio of RMS is equal to 3.61 and 3.41 for EMD and Gaussian smoothing, respectively. The results show that there are several months, for which ratio of RMS for EMD are slightly smaller than for Gaussian smoothing. It is caused by the interpolation method that leads to the overestimation of the signal (Wang et al., 2020). Therefore, we noted that EMD can better filter the noise and extract more geophysical signals than Gaussian smoothing method.

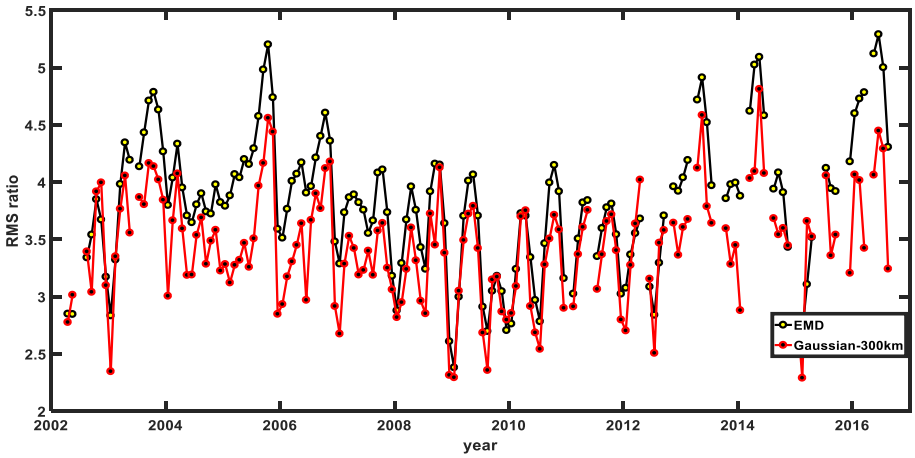

Fig. 8 The ratios of RMS for all available months for EMD and Gaussian 300-km method over the period from April 2002 to August 2016.

4. CONCLUSIONS

In this paper, the empirical mode decomposition method is applied to post-process the monthly temporal gravity field model and compared with the Gaussian smoothing method with the radius of 300 km. The fitting errors of all SH coefficients for the EMD method are almost smaller than those of the Gaussian smoothing method, indicating that EMD can retain more information of the original SH coefficients, especially for the high-degree part. Besides, from the change of the amplitude of each SH coefficient before and after filtering through the spectral domain, we can also find that the EMD method effectively retains more information related to signals than Gaussian smoothing. Almost all ratios of RMS for the EMD method are larger than those of the Gaussian smoothing method, with the mean ratio of RMS 3.61 for EMD, obviously larger than 3.41 for 300 km Gaussian smoothing, which holding that EMD can filter the noise more efficiently and retain more geophysical signals with smaller leakage effect.

ACKNOWLEDGMENTS

This work is mainly funded by the Natural Science Foundation of China (42064001). We acknowledge the GRACE CSR RL06 solutions, which can be downloaded from the website of the International Centre for Global Earth Models (ICGEM) (http://icgem.gfz-potsdam.de).

REFERENCES

Boudraa, A. and Cexus, J.: 2007, EMD-based signal filtering. IEEE Trans. Instrum. Meas., 56, 6, 2196–2202. DOI: 10.1109/TIM.2007.907967

Braun, S. and Feldman, M.: 2011, Decomposition of non-stationary signals into varying time scales: Some aspects of the EMD and HVD methods. Mech. Syst. Signal Process., 25, 7, 2608–2630. DOI: 10.1016/j.ymssp.2011.04.005

Cazenave, A. and Chen, J.: 2010, Time-variable gravity from space and present-day mass redistribution in the Earth system. Earth Planet. Sci. Lett., 298, 3-4, 263–274. DOI: 10.1016/j.epsl.2010.07.035

Chambers, D.P. and Bonin, J.A.: 2012, Evaluation of Release-05 GRACE time-variable gravity coefficients over the ocean. Ocean Sci., 8, 5, 859–868. DOI: 10.5194/os-8-859-2012

Chen, J., Wilson, C., Blankenship, D. et al.: 2009, Accelerated Antarctic ice loss from satellite gravity measurements. Nat. Geosci., 2, 12, 859–862. DOI: 10.1038/ngeo694

Chen, J., Wilson, C. and Seo, K.W.: 2006, Optimized smoothing of Gravity Recovery and Climate Experiment (GRACE) time-variable gravity observations. J. Geophys. Res., Solid Earth, 111, B6, B06408. DOI: 10.1029/2005JB004064

Chen, J.L., Wilson, C.R., Tapley, B.D. et al.: 2007, GRACE detects coseismic and post-seismic deformation from the Sumatra-Andaman Earthquake. Geophys. Res. Lett., 34, L13302. DOI: 10.1029/2007GL030356

Colominas, M., Schlotthauer, G. and Torres, M.: 2014, Improved complete ensemble EMD: A suitable tool for biomedical signal processing. Biomed. Signal Process. Control, 14, 1, 19–29. DOI: 10.1016/j.bspc.2014.06.009

Cui, L., Song. Z., Zou, Z., Xu, W., Wang, X. and Li, Q.: 2019, Analysis of Fan Filtering Algorithm of Gravity Satellite Time-varying Gravitational Potential Coefficient Error. Science Technology and Engineering, 19, 15, 46-51, (in Chinese).

Cui, L., Tang, X., Zou, Z., Song, Z. and Xu, W.: 2020, Parameter Selection in De-correlation Filter Algorithm for Gravity Satellite Time-Variable Gravity Field. Science Technology and Engineering, 20, 1, 43–47, (in Chinese).

Duan, X.J., Guo, J.Y., Shum, C.K. et al.: 2009, On the postprocessing removal of correlated errors in GRACE temporal gravity field solutions. J. Geod., 83, 11, 1095-1106. DOI 10.1007/s00190-009-0327-0

Feng, X., Zhong, J., Yan, R. et al.: 2022, Groundwater radon precursor anomalies identification by EMD-LSTM Model. Water, 14, 1, 69. DOI: 10.3390/w14010069

Frappart, F., Ramillien, G., Leblanc, M. et al.: 2011, An independent component analysis filtering approach for estimating continental hydrology in the GRACE

gravity data. Remote Sens. Environ., 115, 1, 187–204. DOI: 10.1016/j.rse.2010.08.017

Fu, Q., Liu, D., Li, T. et al.: 2016, EMD-RBFNN coupling prediction model of complex regional groundwater depth series: A case study of the Jiansanjiang administration of Heilongjiang land reclamation in China. Water, 8, 8, 340. DOI: 10.3390/w8080340

Gao, C., Lu, Y., Zhang, Z. et al.: 2015, Ice sheet mass balance in Antarctica measured by GRACE and its uncertainty. Chinese J. Geophys., 58, 3, 780–792, (in Chinese, with English Abstract). DOI: 10.6038/cjg20150308

Guo, J., Li, W., Chang, X. et al.: 2018, Terrestrial water storage changes over Xinjiang extracted by combining Gaussian filter and multichannel singular spectrum analysis from GRACE. Geophys. J. Int., 213, 1, 397–407. DOI: 10.1093/gji/ggy006

Guo, J., Mu, D., Liu, X. et al.: 2014, Equivalent water height extracted from GRACE gravity field model with robust independent component analysis. Acta Geophys., 62, 4, 953–972. DOI: 10.2478/s11600-014-0210-0

Guo, F., Sun, Z., Wang, F. et al.: 2018, Review of GRACE satellites time-variable gravity filtering methods. Progress in Geophysics, 33, 5, 1783–1788, /in Chinese). DOI: 10.6038/pg2018BB0393

Huang, N., Shen, Z., Long, S. et al.: 1998, The empirical mode decomposition and the Hilbert spectrum for nonlinear and non-stationary time series analysis. Proc. R. Soc. London A Math. Phys. Eng. Sci., 454, 1971, 903–995. DOI: 10.1098/rspa.1998.0193

Kaihatu, J.M., Handler, R.A., Marmorino, G.O. et al.: 1998, Empirical orthogonal function analysis of ocean surface currents using complex and real-vector methods. J. Atmos. Ocean. Technol., 15, 4, 927–941. DOI: 10.1175/1520-0426(1998)015

Kusche, J.: 2007, Approximate decorrelation and non-isotropic smoothing of time-variable GRACE-type gravity field models. J. Geod., 81, 11, 733–749. DOI: 10.1007/s00190-007-0143-3

Lan, W.H., Kuo, C.Y., Lin, L.C. et al.: 2021, Annual Sea Level Amplitude Analysis over the North Pacific Ocean Coast by Ensemble Empirical Mode Decomposition Method. Remote Sens., 13, 4, 730. DOI: 10.3390/rs13040730

Lei, Y., Lin, J., He, Z. et al.: 2013, A review on empirical mode decomposition in fault diagnosis of rotating machinery. Mech. Syst. Signal Process., 35,1-2, 108–126. DOI: 10.1016/j.ymssp.2012.09.015

Lu, F., You, W., Fan, D. et al.: 2015, Inversion of water storage and seawater quality changes in mainland China in recent 10 years from GRACE RL05 data. Journal of Surveying and Mapping, 44, 2, 160, (in Chinese).

Miao, Q., Wang, D. and Pecht, M.: 2011, Rolling element bearing fault feature extraction using EMD-based independent component analysis. IEEE Conference on Prognostics and Health Management, Denver.

Qian, C., Wu, Z., Fu, C. et al.: 2010, On multi-timescale variability of temperature in China in modulated annual cycle reference frame. Adv. Atmos. Sci., 27, 5, 1169–1182. DOI: 10.1007/s00376-009-9121-4

Ramillien, G., Famiglietti, J.S. and Wahr, J.: 2008, Detection of continental hydrology and glaciology signals from GRACE: a review. Surv. Geophys., 29, 4, 361–374. DOI: 10.1007/s10712-008-9048-9

Rangelova, E., Sideris, M.G. and Kim, J.W.: 2012, On the capabilities of the multi-channel singular spectrum method for extracting the main periodic and non-periodic variability from weekly GRACE data. J. Geod., 54, 64–78. DOI: 10.1016/j.jog.2011.10.006

Rangelova, E., Van der Wal, W., Braun, A. et al.: 2007 Analysis of Gravity Recovery and Climate Experiment time-variable mass redistribution signals over North America by means of principal component analysis. J. Geophys. Res., Earth Surface, 112, F3. DOI: 10.1029/2006JB004605

Schmidt, R., Petrovic, S., Güntner, A. et al.: 2008, Periodic components of water storage changes from GRACE and global hydrology models. J. Geophys. Res., Solid Earth, 113, B8. DOI: 10.1029/2007JB005363

Shen, Y., Wang, F., and Chen, Q.: 2021, Weighted multichannel singular spectrum analysis for post-processing GRACE monthly gravity field models by considering the formal errors. Geophys. J. Int., 226, 3, 1997–2010. DOI: 10.1093/gji/ggab199

Shu, G. and Liang, X.: 2007, Identification of complex diesel engine noise sources based on coherent power spectrum analysis. Mech. Syst. Signal Process., 21, 1, 405–416. DOI: 10.1016/j.ymssp.2006.06.001

Swenson, S. and Wahr, J.: 2006. Post-processing removal of correlated errors in GRACE data. Geophys. Res. Lett., 33, 8, L08402. DOI: 10.1029/2005GL025285

Velicogna, I. and Wahr, J.: 2013, Time-variable gravity observations of ice sheet mass balance: Precision and limitations of the GRACE satellite data. Geophys. Res. Lett., 40, 12, 3055–3063. DOI: 10.1002/grl.50527

Wahr, J., Molenaar, M. and Bryan, F.: 1998, Time variability of the Earth's gravity field: Hydrological and oceanic effects and their possible detection using GRACE. J. Geophys. Res., Solid Earth, 103, B12, 30205–30229. DOI: 10.1029/98JB02844

Wang, L., Chen, C., Zou, R. et al.: 2014: Using GPS and GRACE to detect seasonal horizontal deformation caused by loading of terrestrial water : A case study in the Himalayas. Chin. J. Geophys., 57, 6, 1792–1804, (in Chinese). DOI: 10.6038/cjg20140611

Wang, F., Shen, Y., Chen, T. et al.: 2020, Improved multichannel singular spectrum analysis for post-processing GRACE monthly gravity field models. Geophys. J. Int., 223, 2, 825–839. DOI: 10.1093/gji/ggaa339

Weare, B.C. and Nasstrom, J.S.: 1982, Examples of extended empirical orthogonal function analyses. Mon. Weather Rev., 110, 6, 481–485. DOI: 10.1175/1520-0493(1982)110

Wu, Z., Schneider, E.K., Kirtman, B.P. et al.: 2008, The modulated annual cycle: an alternative reference frame for climate anomalies. Clim. Dyn., 31, 7, 823–841. DOI: 10.1007/s00382-008-0437-z

Yi, S. and Sneeuw, N.: 2022, A novel spatial filter to reduce north–south striping noise in GRACE spherical harmonic coefficients. J. Geod., 96, 23. DOI: 10.1007/s00190-022-01614-z

Zhang, Z., Chao, B., Lu, Y. et al.: 2009, An effective filtering for GRACE time-variable gravity: Fan filter. Geophys. Res. Lett., 36, L17311. DOI: 10.1029/2009GL039459

Zhang, S., He, Y., Li, Z. et al.: 2017, EMD for GPS time series noise reduction analysis. Geod. Geodyn., 37, 12, 1248–1252.

Zou, Z., Song, Z., Cui, L., Tang, X., Xu, W. and Li, L.: 2019, Weighted Average Filtering Algorithm for Banding Error of Gravity Satellite Time-varying Gravity Field. Science Technology and Engineering, 19, 32, 52–57, (in Chinese).